Communications

Role of Surface Iron in Enhanced Activity for the Oxygen Reduction Reaction on a Pd$_3$Fe(111) Single-Crystal Alloy**

Xiaofang Yang, Jun Hu, Jie Fu, Ruqian Wu, and Bruce E. Koel

Dedicated to the Fritz Haber Institute, Berlin, on the occasion of its 100th anniversary

Applications of polymer electrolyte membrane fuel cells (PEM-FCs) require a continued search for an optimal catalyst with attributes of high activity, durability, low cost, and resistance to negative effects of impurities in the fuel. Platinum-based bimetallic catalyst systems are widely utilized in PEM-FCs because of their good performance in both the cathode and the anode.[1–6] Alloying with inexpensive metals can reduce the loading of platinum and lower the cost of the fuel cell, and in some cases the catalytic activity is maintained or even becomes higher. Surprisingly, some non-platinum-based alloy catalysts (e.g., palladium–iron and palladium–cobalt) appear to have even better performance than platinum-based alloy catalysts.[7,8] Recently, higher electrocatalytic activity and stability were observed when metals or alloys were used as supports for a platinum or palladium monolayer.[9–15] Development of improved cathode catalysts would be aided by a fundamental understanding of the oxygen reduction reaction (ORR) mechanism. However, the ORR system is complex and ultimately requires considering fully the effects of water, solvent ions, changing electrical potentials, and a detailed description of the composition and structure of all the chemical phases present at the electrode surface. Thus, progress has been limited in elucidating the origin of the enhanced performance of various bimetallic catalysts. An important factor that can be isolated is the surface composition and structure of the alloy responsible for the ORR kinetics. Herein, we report studies on a bimetallic alloy single crystal, Pd$_3$Fe(111), that combine surface analytical techniques including low-energy ion scattering (LEIS) and scanning tunneling microscopy (STM), electrochemical analysis, and quantum chemistry calculations to investigate the origin of the enhanced ORR properties of Pd–Fe alloys at a molecular level. We find excellent ORR performance for the Pd$_3$Fe(111) crystal after heating to high temperatures in ultrahigh vacuum (UHV) and establish a strong correlation of this performance to the presence of surface Fe atoms.

The lower surface energy of Pd causes significant Pd segregation to the topmost surface layer of Pd–Fe alloys.[16] Pd$_3$Fe(111) surfaces with different structures can be prepared by heating at different temperatures in UHV, and two surface structures are shown by STM images in Figure 1. These two surfaces were studied for catalyzing the oxygen reduction reaction.
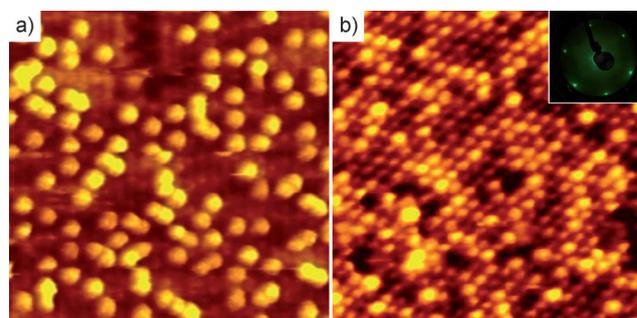

Figure 1. STM constant-current topography images of clean Pd$_3$Fe(111) surfaces illustrating the importance of annealing temperature on surface structure. a) After heating to 1200 K. Image: 7.0×7.0 nm². Tunneling parameters: 1.03 mV, 2.04 nA. High-temperature annealing created Pd monomer and dimer adatoms at the surface. Bright spots are primarily due to segregated Pd monomers and dimers. b) After heating to 1000 K. Image: 7.0×7.0 nm². Tunneling parameters: −302 mV, 340 pA. The Pd adatom features did not form at the lower annealing temperature. Two distinct corrugations are observed, which are due to chemical contrast between Pd and Fe atoms. Bright spots are assigned to Fe atoms. Inset: low-energy electron diffraction pattern at $E_p = 55$ eV.

Curves 1 and 2 in Figure 2 show the cyclic voltammograms (CVs) of Pd$_3$Fe(111) in argon-purged acid electrolyte after the crystal was annealed at 1000 and 1250 K, respectively. The heating caused apparent changes in both hydrogen adsorption/desorption (H$_{ads/des}$) and surface oxide formation/reduction (oxide$_{form/red}$) features at 0.10-0.35 V and 0.65-0.90 V, respectively. A larger area under the H$_{ads/des}$ curves was obtained on Pd$_3$Fe(111) annealed at 1250 K, and we attribute this behavior to the formation of Pd adatoms, which increased the number of surface active sites.[16] The ORR activities of these two Pd$_3$Fe(111) surfaces were measured by sweep voltammetry in O$_2$-saturated HClO$_4$ electrolyte using a rotating-disk electrode at room temperature. Both surfaces
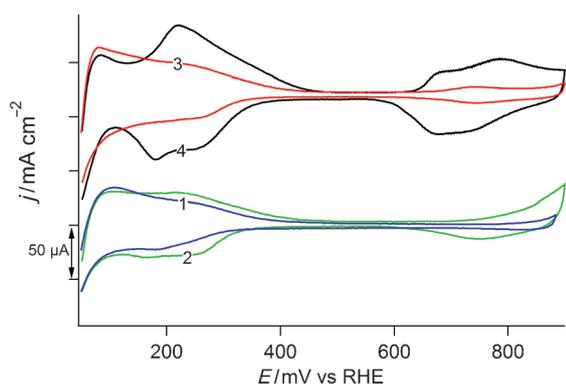
[*] Prof. B. E. Koel
Department of Chemical and Biological Engineering
Princeton University, Princeton, NJ 08544 (USA)
E-mail: bkoel@princeton.edu
Homepage: http://www.princeton.edu/cbe/people/faculty/koel/
Dr. X. Yang, J. Fu
Chemistry Department
Lehigh University, Bethlehem, PA 18015 (USA)
Dr. J. Hu, Prof. R. Wu
Department of Physics and Astronomy
University of California, Irvine, Irvine, CA 92697 (USA)

Supporting information for this article is available on the WWW under http://dx.doi.org/10.1002/anie.201101251.

Figure 2. Voltammetric curves for four different $Pd_3Fe(111)$ surfaces at 300 K in an Ar-purged 0.1 M $HClO_4$ solution. The sweep rate was 20 mVs^{-1}. 1) $Pd_3Fe(111)$, 1000 K, 2) $Pd_3Fe(111)$, 1250 K, 3) Pd ML/$Pd_3Fe(111)$, 4) sputtered $Pd_3Fe(111)$.

were found to be highly active in the ORR with only a small difference. This result indicates that the surface structure of Pd is not the determining factor in controlling the alloy catalytic activity. Pd adatoms may not be stable in acid solution and so dissolve or be transferred to islands or defects. We noted that both alloy surfaces have similar amounts of surface Fe (ca. 10%), so we proposed that this surface Fe plays an important role in the ORR kinetics.

To examine the effect of surface Fe, two other Pd–Fe surfaces were prepared in UHV, one containing a higher Fe concentration of 25% and one that was free of Fe, denoted as sputtered $Pd_3Fe(111)$ and Pd ML/$Pd_3Fe(111)$, respectively. LEIS for all Pd–Fe surfaces before and after electrochemical measurements are shown in Figure 3. The surfaces with 25% Fe were not stable in the electrochemical environment, and surface Fe was dissolved slowly in the electrolyte during polarization scanning. However, no substantial change was
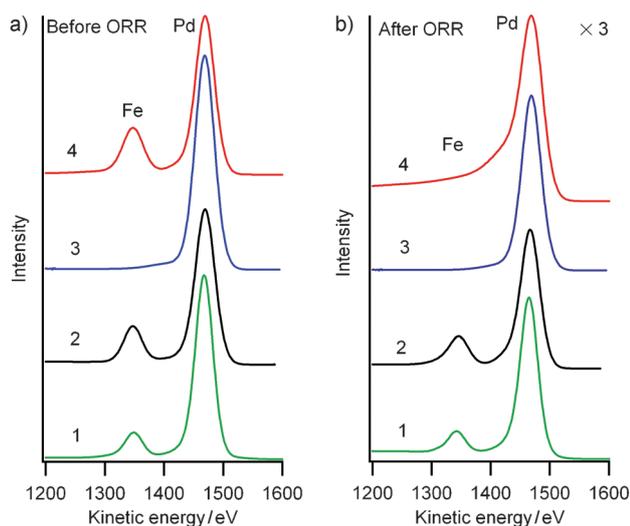
detected in surface Fe concentration after electrochemical measurements for the annealed $Pd_3Fe(111)$ surfaces with 10% or less surface Fe. (See Figures S1 and S2 in Supporting Information regarding surface Fe concentrations.) Therefore, surface geometry and composition has an important effect on the stability of surface Fe. As shown in Figure 2, which gives the CVs for all Pd–Fe surfaces in O_2-free electrolyte, the large increase of the $H_{ads/des}$ peaks in curve 4 is due to H adsorption/desorption from the near surface layers after depletion of surface Fe. Increases in the onset potentials for surface oxide$_{form/red}$ and decreases in the onset potentials for $H_{ads/des}$ were observed for all of the annealed $Pd_3Fe(111)$ surfaces.

ORR polarization curves for Pd–Fe surfaces are plotted and compared to Pd(111) and Pt(111) in Figure 4. The corresponding ORR kinetic parameters are given in Supporting Information Table S1. Mechanically polished Pd(111) (not shown) had the worst ORR activity, similar to that of the polished $Pd_3Fe(111)$ surface.[10] Slight improvement was observed for sputtered $Pd_3Fe(111)$. Apparently, pure Pd(111) or rough $Pd_3Fe(111)$ surfaces are not good ORR catalysts. However, the formation of a Pd monolayer, denoted as Pd ML/$Pd_3Fe(111)$, significantly increased the ORR activity to a level of performance comparable to Pt(111), which is consistent with the report by Adzic et al.[10] Interestingly, the highest ORR activity was obtained on the $Pd_3Fe(111)$ surface that had been heated to 1250 K. This surface had a $E_{1/2}$ value 27 mV more positive than Pd ML/$Pd_3Fe(111)$ and 62 mV more positive than Pd(111). The kinetic current density for the $Pd_3Fe(111)$ alloy annealed at 1250 K is two to three times larger than that from Pd ML/$Pd_3Fe(111)$ and five to eight times larger than that for annealed Pd(111) in the potential range of 0.80–0.90 V. Detailed analysis of all oxygen polarization curves are supplied in the Supporting Information Figures S4–S7. Our study strongly indicates that an optimal surface concentration of approximately 10% Fe is needed to have high ORR activity.

First-principles calculations based on density functional theory (DFT) were performed to explore O_2 adsorption and reaction on two different Pd–Fe surfaces. One was a Pd ML/
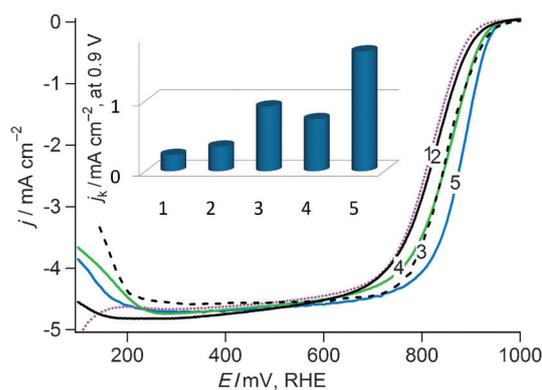

Figure 3. LEIS spectra for $Pd_3Fe(111)$ surfaces. a) Before ORR. b) After ORR. LEIS conditions: 1.6 keV He$^+$, 3.0 nA. ORR conditions: 15 polarization scans between 0 to 1000 mV in an O_2-purged 0.1 M $HClO_4$ solution. 1) $Pd_3Fe(111)$, 1000 K, 2) $Pd_3Fe(111)$, 1250 K, 3) Pd ML/$Pd_3Fe(111)$, 4) sputtered $Pd_3Fe(111)$.

Figure 4. ORR polarization curves for several $Pd_3Fe(111)$, Pd(111), and Pt(111) surfaces. Polarization curves were obtained at 300 K in an O_2-purged 0.1 M $HClO_4$ solution with a sweep rate of 20 mVs^{-1} and rotation rate of 900 rpm. 1) Pd(111), 2) sputtered $Pd_3Fe(111)$, 3) Pt(111), 4) Pd ML/$Pd_3Fe(111)$, 5) annealed $Pd_3Fe(111)$. Inset: Kinetic current at 0.9 V.

Pd$_3$Fe(111) (surface I) and the other was a Pd$_3$Fe(111) alloy with a low Fe concentration of 6.25% at the surface (surface II). Details of DFT calculations are provided in the Supporting Information. The adsorption energies of O$_2$ molecules on surface I and surface II are 0.74 and 1.24 eV, respectively. These results reflect a stronger interaction between Fe and O$_2$ than between Pd and O$_2$, which benefits the first electron and proton transfer, M$-$O$_2$ + H$^+$ + e$^-$ → M$-$OOH (where M is the reaction site), a possible rate-determining step.[17] The dissociation of O$_2$ on surface II is much easier than on surface I, with an energy barrier of 0.28 eV compared to 1.02 eV from the energy profiles plotted in Figure 5. This result clearly indicates the great benefit of having surface Fe for oxygen dissociation, consistent with our experimental observations.

There is still considerable controversy about the detailed reaction mechanism in ORR, but it has been agreed that the rate-determining step in ORR is either molecular oxygen dissociation, first electron and proton transfer, or removal of surface oxygen ad-species.[18] It has been recognized that the Pd monolayer on Pd$_3$Fe(111) has different electronic properties from pure Pd, which causes a large difference in ORR activity between these two surfaces. The Pd monolayer on Pd$_3$Fe(111) has a d-band center shifted down by 0.25 eV compared to Pd(111), which significantly lowers the binding energy of O and OH to the surface and thus improves the removal of O and OH by protonation.[7] The presence of 10% randomly distributed surface Fe on the high-temperature annealed Pd$_3$Fe(111) causes inhomogeneity in both surface structure and composition, which makes it difficult to explain the catalytic activity simply by the d-band shifting. Because of the small amount of Fe and large amount of Pd on the Pd$_3$Fe(111) surface, it is possible that a synergistic effect exists to take advantage of the capability of Fe sites for strong oxygen adsorption/dissociation and the capability of the Pd layer for fast removal of oxygen species by protonation. This process requires the spillover of oxygen species from Fe sites to Pd sites, and it would be strongly affected by the diffusion barriers of oxygen species over the surface. Our calculations (Figure 5) show that after O$_2$ dissociation at the Fe site, one O

atom can diffuse easily across areas with pure Pd (represented by the diffusion of O1) with a small energy barrier of 0.25 eV. In contrast, the barrier for the second O atom to diffuse away from the Fe atom (represented by the diffusion of O2) is as high as 1.25 eV. This high barrier may result in irreversible adsorption of an oxygen atom to the Fe site, causing site-blocking of further reactions. Intriguingly, this pre-adsorbed O atom does not hinder further O$_2$ dissociation at the corresponding Fe site at all, and the energy barrier is 0.40 eV. Furthermore, the follow-up O diffusion out of the surface Fe region is significantly promoted, with the energy barrier decreasing from 1.25 to 0.75 eV (Supporting Information, Figure S8). Therefore, partial covering of O atoms near surface Fe not only preserves high activity of O$_2$ dissociation but also enhances the O atom diffusion near surface Fe. This feature could balance the O$_2$ dissociation and O diffusion, so that the ORR process continues dynamically at a high rate.

A better understanding of the ORR mechanism at this surface requires more detailed modeling of the many possible reaction pathways, which is very complicated and beyond the scope of this Communication. However, we believe that presence of active metal elements that significantly enhance molecular oxygen adsorption and dissociation and Pd surface segregation that lowers the O binding energy to the surface are important factors that influence ORR kinetics on Pd-based alloys. Furthermore, this study suggests a possible oxygen spillover mechanism between different elements at the binary alloy surface.[19] It should be worth studying the enhanced ORR performance considering this mechanism for other alloy electrocatalytic systems, such as Pt/Pd, Pt/Ir, and so forth.

In summary, we have prepared a Pd$_3$Fe(111) alloy single crystal in UHV with different surface compositions and morphologies and investigated the performance of these surfaces as cathode catalysts. We observed a strong correlation of the electrocatalytic activity with the surface Fe concentration, with the highest performance at approximately 10% Fe. The Pd$_3$Fe(111) surfaces prepared by high-temperature heating in UHV were found to be five to eight times more active than Pd(111) and twice as active as Pt(111). This study not only demonstrates Pd–Fe to be a possible candidate to replace Pt as the cathode electrocatalyst but also points out the important role of small amounts of active elements in non-Pt alloy electrocatalysts. The presence of surface Fe atoms largely impacts both O$_2$ adsorption and O$_2$ dissociation, which are important, perhaps rate-determining, steps in ORR. We are aware that the long-term stability of active-metal-modified alloys is questionable and should be evaluated by a different study.
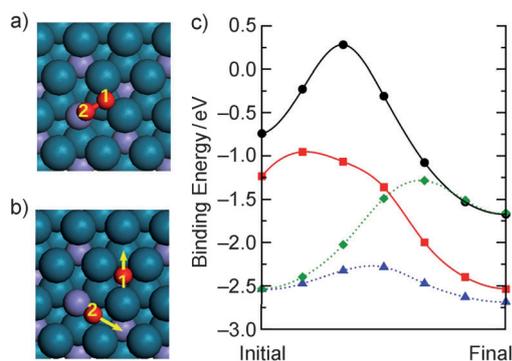
Figure 5. a,b) Top views of the O$_2$ adsorption configuration (a) and O$_2$ dissociation configuration (b) on surface II. Large, medium, and small spots denote Pd, Fe, and O atoms, respectively. Arrows indicate the diffusion pathways of O1 and O2. c) Energy profiles for dissociation of O$_2$ (● surface I, ■ surface II) and diffusion of O1 (▲) and O2 (◆).

[1] A. Kowal, M. Li, M. Shao, K. Sasaki, A. I. Frenkel, R. R. Adzic, *Nat. Mater.* **2009**, *8*, 325.

[2] I. J. Hsu, D. A. Hansgen, B. E. McCandless, B. G. Willis, J. G. Chen, *J. Phys. Chem. C* **2011**, *115*, 3709.

[3] V. R. Stamenkovic, B. S. Mun, M. Arenz, K. J. J. Mayrhofer, C. A. Lucas, G. Wang, P. N. Ross, N. M. Markovic, *Nat. Mater.* **2007**, *6*, 241.

[4] S. Chen, W. Sheng, N. Yabuuchi, P. J. Ferreira, L. F. Allard, Y. Shao-Horn, *J. Phys. Chem. C* **2009**, *113*, 1109.

[5] V. R. Stamenkovic, B. Fowler, B. S. Mun, G. Wang, P. N. Ross, C. A. Lucas, N. M. Markovic, *Science* **2007**, *315*, 493.

[6] L. Xiong, A. Manthiram, *J. Electrochem. Soc.* **2005**, *152*, A697.

[7] M. Shao, P. Liu, J. Zhang, R. Adzic, *J. Phys. Chem. B* **2007**, *111*, 6772.

[8] M.-H. Shao, K. Sasaki, R. R. Adzic, *J. Am. Chem. Soc.* **2006**, *128*, 3526.

[9] V. R. Stamenkovic, B. S. Mun, K. J. J. Mayrhofer, P. N. Ross, N. M. Markovic, *J. Am. Chem. Soc.* **2006**, *128*, 8813.

[10] W.-P. Zhou, X. Yang, M. B. Vukmirovic, B. E. Koel, J. Jiao, G. Peng, M. Mavrikakis, R. R. Adzic, *J. Am. Chem. Soc.* **2009**, *131*, 12755.

[11] R. Adzic, J. Zhang, K. Sasaki, M. Vukmirovic, M. Shao, J. Wang, A. Nilekar, M. Mavrikakis, J. Valerio, F. Uribe, *Top. Catal.* **2007**, *46*, 249.

[12] J. Zhang, M. B. Vukmirovic, Y. Xu, M. Mavrikakis, R. R. Adzic, *Angew. Chem.* **2005**, *117*, 2170; *Angew. Chem. Int. Ed.* **2005**, *44*, 2132.

[13] P. Hirunsit, P. B. Balbuena, *J. Phys. Chem. C* **2010**, *114*, 13055.

[14] K. Sasaki, H. Naohara, Y. Cai, Y. M. Choi, P. Liu, M. B. Vukmirovic, J. X. Wang, R. R. Adzic, *Angew. Chem.* **2010**, *122*, 8784; *Angew. Chem. Int. Ed.* **2010**, *49*, 8602.

[15] R. Yang, J. Leisch, P. Strasser, M. F. Toney, *Chem. Mater.* **2010**, *22*, 4712.

[16] X. Yang, J. Hu, R. Wu, B. E. Koel, *J. Phys. Chem. Lett.* **2010**, *1*, 2493.

[17] A. Panchenko, M. T. M. Koper, T. E. Shubina, S. J. Mitchell, E. Roduner, *J. Electrochem. Soc.* **2004**, *151*, A2016.

[18] J. K. Nørskov, J. Rossmeisl, A. Logadottir, L. Lindqvist, J. R. Kitchin, T. Bligaard, H. Jónsson, *J. Phys. Chem. B* **2004**, *108*, 17886.

[19] J. L. Fernández, D. A. Walsh, A. J. Bard, *J. Am. Chem. Soc.* **2005**, *127*, 357.